Spectral shift of a twisted electromagnetic Gaussian Schell-model beam focused by a thin lens

S. Zhu · Y. Cai

Abstract Spectral changes of a twisted electromagnetic Gaussian Schell-model (EGSM) beam focused by a thin lens are investigated by using a tensor method. It is shown that the spectral shift is mainly determined by the degree of polarization, twist phase and correlation coefficients of the initial beam. Generically the blue shift occurs at on-axis points, while the red shift can occur at off-axis points.

1 Introduction

In the past decades, partially coherent beams have found wide applications in inertial confinement fusion, optical imaging, optical projection, laser scanning, photography, free-space optical communications, nonlinear optics and optical trapping [1], etc. Gaussian Schell-model (GSM) beam is a typical partially coherent beam whose spectral degree of coherence and the intensity distribution are Gaussian functions [2–7]. A more general partially coherent beam can possess a twist phase. The twisted GSM beam was introduced by Simon and Mukunda [8]. The twist phase differs in many respects from the ordinary quadratic phase factor [8, 9]. The twist phase rotates the beam spot on propagation due to its intrinsic chiral property and increases the beam divergence on propagation. Propagation, generation, second harmonic generation and ghost imaging of twisted GSM beams have been studied widely [8–22].

In the past decade, stochastic electromagnetic beam has attracted more and more attention owing to its importance in

S. Zhu · Y. Cai (✉)
School of Physical Science and Technology, Soochow University, Suzhou 215006, China
e-mail: yangjian_cai@yahoo.com.cn

theories of coherence and polarization of light and in some applications, e.g., free-space optical communications [23–43]. Electromagnetic GSM beam was introduced as an extension of scalar GSM beam [26–28]. Numerous theoretical and experimental papers have been published on propagation, generation and application of electromagnetic GSM beams [26–41]. It was found that the electromagnetic GSM beam has advantage over a scalar GSM beams (i.e. fully polarized GSM beam) for overcoming the destructive effect of atmospheric turbulence, and have important potential application in free-space optical communications [36]. Cai and co-workers studied the evolution of the electromagnetic GSM beams in resonators and in radar systems operating through the turbulent atmosphere with the help of a tensor method [37–41]. More recently, Cai and Korotkova introduced twisted electromagnetic GSM beam, and studied its propagation in free space [42] and its radiation force on a Rayleigh dielectric particle [43].

In 1986 Wolf found that the spectrum of the light emitted from a spatially partially coherent source with a wide spectral bandwidth may exhibit a shift on propagation in free space [44]. Since then, correlation-induced spectral changes have been studied extensively [44–54]. The spectral changes of scalar GSM and twisted GSM beams focused by a thin lens were studied in [52–54]. To our knowledge no results have been reported up until now on spectral changes of an electromagnetic GSM beam with or without twist phase focused by a thin lens. In fact, up to now, only few papers were published on the spectral changes of stochastic electromagnetic beams [55–58]. This paper is aimed to investigate the spectral shift of an electromagnetic twisted GSM beam focused by a thin lens.

2 Theory

Based on the unified theory of coherence and polarization, the second-order statistical properties of the stochastic electromagnetic beam can be characterized by the cross-spectral density matrix of the electric field, defined by the formula [23–28]

$$
\overset{\leftrightarrow}{\mathbf{W}}(\mathbf{r}_1, \mathbf{r}_2, 0, \omega)
$$

$$
= \begin{pmatrix} W_{xx}(\mathbf{r}_1, \mathbf{r}_2, 0, \omega) & W_{xy}(\mathbf{r}_1, \mathbf{r}_2, 0, \omega) \\ W_{yx}(\mathbf{r}_1, \mathbf{r}_2, 0, \omega) & W_{yy}(\mathbf{r}_1, \mathbf{r}_2, 0, \omega) \end{pmatrix}, \tag{1}
$$

with elements

$$
W_{\alpha\beta}(\mathbf{r}_1, \mathbf{r}_2, 0, \omega) = \langle E_\alpha^*(\mathbf{r}_1, 0, \omega) E_\beta(\mathbf{r}_2, 0, \omega) \rangle
$$

$$
(\alpha = x, y; \beta = x, y), \tag{2}
$$

where E_x and E_y denote the components of the random electric vector, at frequency ω, with respect to two mutually orthogonal, x and y directions, perpendicular to the z-axis. The "*" denotes the complex conjugate and the angular brackets denote ensemble average.

For a twisted electromagnetic GSM beam, its element $W_{\alpha\beta}(\mathbf{r}_1, \mathbf{r}_2, 0, \omega)$ is expressed as [42]

$$
W_{\alpha\beta}(\mathbf{r}_1, \mathbf{r}_2, 0, \omega)
$$

$$
= \sqrt{S_\alpha(\mathbf{r}_1, 0, \omega)} \sqrt{S_\beta(\mathbf{r}_2, 0, \omega)} \mu_{\alpha\beta}(\mathbf{r}_1 - \mathbf{r}_2, 0, \omega)
$$

$$
\times \exp\left[-\frac{ik}{2} \gamma_{\alpha\beta}(\mathbf{r}_1 - \mathbf{r}_2)^T \mathbf{J}(\mathbf{r}_1 + \mathbf{r}_2) \right]
$$

$$
(\alpha = x, y; \beta = x, y), \tag{3}
$$

where

$$
S_\alpha(\mathbf{r}_1, 0, \omega) = \frac{A_\alpha^2 \Gamma_0^2}{(\omega - \omega_0)^2 + \Gamma_0^2} \exp\left(-\frac{\mathbf{r}_1^2}{2\sigma_\alpha^2} \right) \quad (\alpha = x, y)
$$

denotes the spectral density of the component $E_\alpha(\mathbf{r}_1, 0, \omega)$ of the electric vector (here we have assumed that the initial spectrum of the component $E_\alpha(\mathbf{r}_1, 0, \omega)$ is of the Lorentz type) with ω_0 being the central frequency and Γ_0 being the half-width at half-maximum, ω is the angular frequency, σ_α is the r.m.s. width of the spectral density along α direction, $k = \omega/c$ is the wave number with c being the velocity of light in vacuum;

$$
\mu_{\alpha\beta}(\mathbf{r}_1 - \mathbf{r}_2, 0, \omega) = B_{ij} \exp\left[-\frac{(\mathbf{r}_1 - \mathbf{r}_2)^2}{2\delta_{\alpha\beta}^2} \right]
$$

$$
(\alpha = x, y; \beta = x, y)
$$

is the degree of correlation between the components $E_\alpha(\mathbf{r}_1, 0, \omega)$ and $E_\beta(\mathbf{r}_2, 0, \omega)$, δ_{xx}, δ_{yy} and δ_{xy} are the r.m.s. widths of auto-correlation functions of the x component of

the field, of the y component of the field and of the mutual correlation function of x and y field components, respectively, B_{xy} is the complex correlation coefficient between the x and y components of the electric field; Parameters A_α, $B_{\alpha\beta} = |B_{\alpha\beta}| \exp(i\phi_{\alpha\beta}) = B_{\beta\alpha}^*$, σ_α and $\delta_{\alpha\beta}$ are independent of position and, in our analysis, of frequency. The nine real parameters A_x, A_y, σ_x, σ_y, $|B_{xy}|$, ϕ_{xy}, δ_{xx}, δ_{yy} and δ_{xy} entering the general model are shown to satisfy several intrinsic constraints and obey some simplifying assumptions (e.g. the phase difference between the x an y components of the field is removable, i.e. $\phi_{\alpha\alpha} = 0$) [33, 34]. $\gamma_{\alpha\beta}$ represents the twist factor and is limited by $\gamma_{\alpha\beta}^2 \leq 1/(k^2 \delta_{\alpha\beta}^4)$ if $\alpha = \beta$ due to the non-negativity requirement of the cross-spectral density [8, 42]. $\mathbf{J}$ is an anti-symmetric matrix, i.e.,

$$
\mathbf{J} = \begin{pmatrix} 0 & 1 \\ -1 & 0 \end{pmatrix}. \tag{4}
$$

Under the condition of $\gamma_{\alpha\beta} = 0$, (3) reduces to the expression for an element of an electromagnetic GSM beam without twist phase [26–28].

Equation (1) can alternatively be expressed in the following tensor form [15, 42]:

$$
W_{\alpha\beta}(\tilde{\mathbf{r}}, \omega, 0) = \frac{A_\alpha A_\beta B_{\alpha\beta} \Gamma_0^2}{(\omega - \omega_0)^2 + \Gamma_0^2} \exp\left[-\frac{i\omega}{2c} \tilde{\mathbf{r}}^T \mathbf{M}_{0\alpha\beta}^{-1} \tilde{\mathbf{r}} \right]
$$

$$
(\alpha = x, y; \beta = x, y) \tag{5}
$$

with

$$
\mathbf{M}_{0\alpha\beta}^{-1} = \begin{pmatrix} \frac{c}{i\omega}(\frac{1}{2\sigma_\alpha^2} + \frac{1}{\delta_{\alpha\beta}^2})\mathbf{I} & \frac{ci}{\omega\delta_{\alpha\beta}^2}\mathbf{I} + \gamma_{\alpha\beta}\mathbf{J} \\ \frac{ci}{\omega\delta_{\alpha\beta}^2}\mathbf{I} + \gamma_{\alpha\beta}\mathbf{J}^T & \frac{c}{i\omega}(\frac{1}{2\sigma_\beta^2} + \frac{1}{\delta_{\alpha\beta}^2})\mathbf{I} \end{pmatrix}, \tag{6}
$$

where $\mathbf{I}$ is the 2×2 identity matrix, $\tilde{\mathbf{r}} \equiv (\mathbf{r}_1\ \mathbf{r}_2)$, c is the velocity of light in vacuum.

After propagating through a general astigmatic ABCD optical system, the elements of the cross-spectral density matrix can be expressed in the following tensor form [37, 42]:

$$
W_{\alpha\beta}(\tilde{\boldsymbol{\rho}}, \omega, z)
$$

$$
= \frac{A_\alpha A_\beta B_{\alpha\beta} \Gamma_0^2}{(\omega - \omega_0)^2 + \Gamma_0^2} \left[\mathrm{Det}\left(\bar{\mathbf{A}} + \bar{\mathbf{B}}\mathbf{M}_{0\alpha\beta}^{-1} \right) \right]^{-1/2}
$$

$$
\times \exp\left[-\frac{i\omega}{2c} \tilde{\boldsymbol{\rho}}^T \mathbf{M}_{1\alpha\beta}^{-1} \tilde{\boldsymbol{\rho}} \right]
$$

$$
(\alpha = x, y; \beta = x, y) \tag{7}
$$

where Det stands for the determinant of a matrix, $\tilde{\boldsymbol{\rho}} \equiv (\boldsymbol{\rho}_1\ \boldsymbol{\rho}_2)$ with $\boldsymbol{\rho}_1$ and $\boldsymbol{\rho}_2$ being the transverse position vectors in the output plane, while $\mathbf{M}_{1\alpha\beta}^{-1}$ and $\mathbf{M}_{0\alpha\beta}^{-1}$ are related by the following known tensor ABCD law [15]:

$$
\mathbf{M}_{1\alpha\beta}^{-1} = \left(\bar{\mathbf{C}} + \bar{\mathbf{D}}\mathbf{M}_{0\alpha\beta}^{-1} \right)\left(\bar{\mathbf{A}} + \bar{\mathbf{B}}\mathbf{M}_{0\alpha\beta}^{-1} \right)^{-1}. \tag{8}
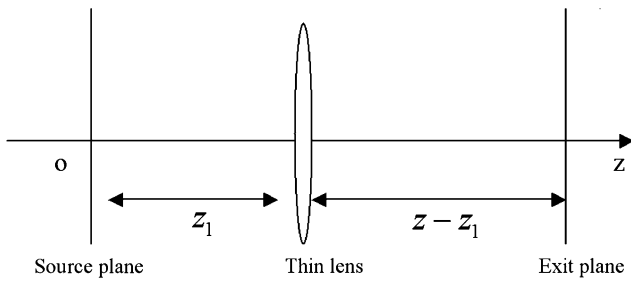$$

Fig. 1 Focusing geometry

Here $\bar{\mathbf{A}}$, $\bar{\mathbf{B}}$, $\bar{\mathbf{C}}$ and $\bar{\mathbf{D}}$ are 4×4 matrices of the form:

$$\bar{\mathbf{A}} = \begin{pmatrix} \mathbf{A} & 0\mathbf{I} \\ 0\mathbf{I} & \mathbf{A}^* \end{pmatrix}, \qquad \bar{\mathbf{B}} = \begin{pmatrix} \mathbf{B} & 0\mathbf{I} \\ 0\mathbf{I} & -\mathbf{B}^* \end{pmatrix},$$

$$\bar{\mathbf{C}} = \begin{pmatrix} \mathbf{C} & 0\mathbf{I} \\ 0\mathbf{I} & -\mathbf{C}^* \end{pmatrix}, \qquad \bar{\mathbf{D}} = \begin{pmatrix} \mathbf{D} & 0\mathbf{I} \\ 0\mathbf{I} & \mathbf{D}^* \end{pmatrix}, \qquad (9)$$

where $\mathbf{A}$, $\mathbf{B}$, $\mathbf{C}$ and $\mathbf{D}$ are the 2×2 sub-matrices of the general astigmatic ABCD optical system, and "*" in (9) is required for an general optical system with loss or gain (e.g., dispersive media, a Gaussian aperture, and helical gas lenses), although it doesn't appears in (13) of Ref. [15].

The focusing geometry is shown in Fig. 1, where the thin lens with focal length f is located at $z = z_1$ and the exit plane is located at z. Here the transformation matrix of the total optical system between the source plane and the exit plane has the form

$$\begin{pmatrix} \mathbf{A} & \mathbf{B} \\ \mathbf{C} & \mathbf{D} \end{pmatrix} = \begin{pmatrix} \mathbf{I} & (z - z_1)\mathbf{I} \\ 0 & \mathbf{I} \end{pmatrix} \begin{pmatrix} \mathbf{I} & 0\mathbf{I} \\ -(1/f)\mathbf{I} & \mathbf{I} \end{pmatrix} \begin{pmatrix} \mathbf{I} & z_1\mathbf{I} \\ 0\mathbf{I} & \mathbf{I} \end{pmatrix}$$

$$= \begin{pmatrix} (1 - Z)\mathbf{I} & (z - z_1 Z)\mathbf{I} \\ -(1/f)\mathbf{I} & (1 - z_1/f)\mathbf{I} \end{pmatrix}, \qquad (10)$$

with $Z = (z - z_1)/f$. The spectral density at the point $\boldsymbol{\rho}$ is then given by the formula

$$S(\boldsymbol{\rho}, z, \omega) \equiv \text{Tr}\,\overset{\leftrightarrow}{\mathbf{W}}(\boldsymbol{\rho}, \boldsymbol{\rho}, z, \omega)$$

$$= W_{xx}(\boldsymbol{\rho}, \boldsymbol{\rho}, z, \omega) + W_{yy}(\boldsymbol{\rho}, \boldsymbol{\rho}, z, \omega). \qquad (11)$$

We can calculate the spectral shift of the twisted electromagnetic GSM beam focused by a thin lens by using (7)–(11).

3 Numerical results

Now we study numerically the spectral shift of a twisted electromagnetic GSM beam focused by a thin lens. For the convenience of analysis, we only consider the twisted electromagnetic GSM beam that is generated by a stochastic
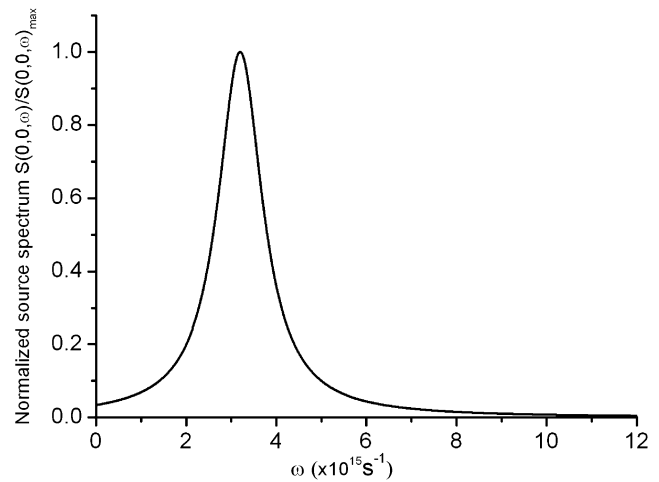

Fig. 2 Normalized source spectrum $S(0, 0, \omega)/S(0, 0, \omega)_{\max}$

electromagnetic source whose the cross-spectral density matrix is diagonal, i.e. of the form

$$\overset{\leftrightarrow}{\mathbf{W}}(\mathbf{r}_1, \mathbf{r}_2, 0, \omega)$$

$$= \begin{pmatrix} W_{xx}(\mathbf{r}_1, \mathbf{r}_2, 0, \omega) & 0 \\ 0 & W_{yy}(\mathbf{r}_1, \mathbf{r}_2, 0, \omega) \end{pmatrix}. \qquad (12)$$

The degree of polarization of the initial source beam at point $\mathbf{r}$ can be expressed as follows [26–28]:

$$P_0(\mathbf{r}, 0, \omega) = \sqrt{1 - \frac{4 \, \text{Det}\,\overset{\leftrightarrow}{\mathbf{W}}(\mathbf{r}, \mathbf{r}, 0, \omega)}{[\text{Tr}\,\overset{\leftrightarrow}{\mathbf{W}}(\mathbf{r}, \mathbf{r}, 0, \omega)]^2}}. \qquad (13)$$

Under the condition of $W_{xx}(\mathbf{r}_1, \mathbf{r}_2, 0, \omega) = 0$ or $W_{yy}(\mathbf{r}_1, \mathbf{r}_2, 0, \omega) = 0$, the twisted electromagnetic GSM beam reduces to a scalar twisted GSM beam with $P_0(\mathbf{r}, 0, \omega) = 1$. In the following numerical examples, we set $\sigma_x = \sigma_y = 3$ mm, $A_x = 1$, $B_{xx} = B_{yy} = 1$, $f = 100$ mm and $z_1 = 200$ mm. In this case, the polarization properties are uniform across the source plane with

$$P_0(\mathbf{r}, 0, \omega) = \left| \frac{A_x^2 - A_y^2}{A_x^2 + A_y^2} \right|,$$

and the degree of polarization at source plane varies as the value of A_y varies. The parameters used in all numerical calculations are set to $\omega_0 = 3.2 \times 10^{15}$ rad/s and $\Gamma_0 = 0.6 \times 10^{15}$ rad/s. Figure 2 shows the normalized source spectrum $S(0, 0, \omega)/S(0, 0, \omega)_{\max}$. We find from Fig. 2 that the frequency of the beam considered in our paper is mainly confined within $0 < \omega < 12 \times 10^{15}$ s^{-1}, although technically all frequencies can be present in the radiation. In all following numerical examples, the values of the twisted parameters γ_{xx} and γ_{yy} have been chosen to satisfy $\gamma_{xx}^2 \leq c^2/(\omega_{\max}^2 \delta_{xx}^4)$ and $\gamma_{yy}^2 \leq c^2/(\omega_{\max}^2 \delta_{yy}^4)$ with $\omega_{\max} = 12 \times 10^{15}$ s^{-1}.
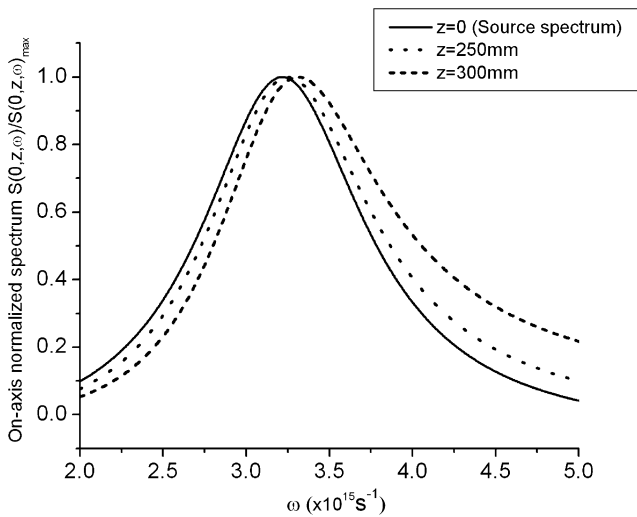
Fig. 3 On-axis normalized spectrum $S(0, z, \omega)/S(0, z, \omega)_{max}$ of a focused electromagnetic GSM beam without twist phase ($\gamma_{xx} = \gamma_{yy} = 0$) at several propagation distances

Fig. 4 On-axis relative spectral shift η of a focused electromagnetic GSM beam without twist phase ($\gamma_{xx} = \gamma_{yy} = 0$) versus propagation distance for different values of the degree of polarization of the initial beam with $\delta_{xx} = 0.01$ mm and $\delta_{yy} = 0.02$ mm

We calculate in Fig. 3 the on-axis normalized spectrum $S(0, z, \omega)/S(0, z, \omega)_{max}$ of a focused electromagnetic GSM beam without twist phase ($\gamma_{xx} = \gamma_{yy} = 0$) at several propagation distances with $P_0 = 0.6$, $\delta_{xx} = 0.01$ mm, $\delta_{yy} = 0.02$ mm. For the convenience of comparison, the source spectrum is also calculated (see solid line of Fig. 3). One finds from Fig. 3 that the spectrum profile of the on-axis normalized spectrum of the focused electromagnetic GSM beam behind the thin lens is similar to the source spectrum, but its peak position is blue-shifted. This phenomenon also occurs for a focused scalar GSM beam as shown in [52–54].

Now we discuss the dependence of the relative spectral shift of a focused electromagnetic GSM beam on its initial degree of coherence and other beam parameters. The spectral shift $\Delta\omega$ is the difference between the peak frequency ω_m of the spectrum of the field after propagation and the peak frequency ω_0 of the source spectrum. A positive value of $\Delta\omega$ denotes a blue shift, while a negative value represents a red shift. We will study the variation of the relative spectral shift, which is defined as

$$\eta = (\omega_m - \omega_0)/\omega_0. \qquad (14)$$

Figure 4 shows the on-axis relative spectral shift η of a focused electromagnetic GSM beam without twist phase ($\gamma_{xx} = \gamma_{yy} = 0$) versus propagation distance for different values of the degree of polarization of the initial beam with $\delta_{xx} = 0.01$ mm and $\delta_{yy} = 0.02$ mm. One finds from Fig. 4 that the maximum relative spectral shift of a focused electromagnetic GSM beam occurs at the back focal plane, while the minimum relative spectral shift (i.e., no spectral shift) occurs at the image plane ($z = 400$ mm). The results are in agreement with the results derived for the case of scalar
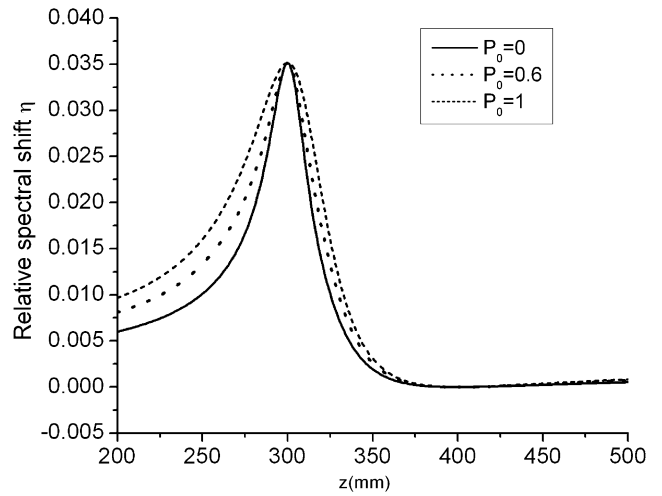
GSM beam [52–54]. It is also evident that the degree of polarization of the initial beam affects the relative spectral shift strongly. The relative spectral shift increases as the degree of polarization increases, while we should note that the position of the maximum relative spectral shift and the position of the zero spectral shift are independent of the degree of polarization.

Now we analyze the properties of the electromagnetic GSM beam at the image plane and the back focal plane, respectively. Substituting (7) and (8) into (10) and by setting $\boldsymbol{\rho}_1 = \boldsymbol{\rho}_2 = \boldsymbol{\rho}$, we obtain

$$S(\boldsymbol{\rho}, z, \omega)$$

$$= \frac{\Gamma_0^2}{(\omega - \omega_0)^2 + \Gamma_0^2} A_x^2 \big[\text{Det}\big(\bar{\mathbf{A}} + \bar{\mathbf{B}}\mathbf{M}_{0xx}^{-1}\big)\big]^{-1/2}$$

$$\times \exp\left[-\frac{i\omega}{2c}\bar{\boldsymbol{\rho}}^T\big(\bar{\mathbf{C}} + \bar{\mathbf{D}}\mathbf{M}_{0xx}^{-1}\big)\big(\bar{\mathbf{A}} + \bar{\mathbf{B}}\mathbf{M}_{0xx}^{-1}\big)^{-1}\bar{\boldsymbol{\rho}}\right]$$

$$+ \frac{\Gamma_0^2}{(\omega - \omega_0)^2 + \Gamma_0^2} A_y^2 \big[\text{Det}\big(\bar{\mathbf{A}} + \bar{\mathbf{B}}\mathbf{M}_{0yy}^{-1}\big)\big]^{-1/2}$$

$$\times \exp\left[-\frac{i\omega}{2c}\bar{\boldsymbol{\rho}}^T\big(\bar{\mathbf{C}} + \bar{\mathbf{D}}\mathbf{M}_{0yy}^{-1}\big)\big(\bar{\mathbf{A}} + \bar{\mathbf{B}}\mathbf{M}_{0yy}^{-1}\big)^{-1}\bar{\boldsymbol{\rho}}\right], \qquad (15)$$

where $\tilde{\boldsymbol{\rho}} \equiv (\boldsymbol{\rho}\ \boldsymbol{\rho})$. If the optical system shown in Fig. 1 satisfies the imaging condition, i.e.,

$$\frac{1}{z_1} + \frac{1}{z - z_1} = \frac{1}{f}, \qquad (16)$$

then we can obtain $\mathbf{B} = 0$. If we set $\boldsymbol{\rho} \equiv (0\ 0)$, (15) reduces to

$$S(0, z, \omega)$$

$$= \frac{\Gamma_0^2}{(\omega - \omega_0)^2 + \Gamma_0^2} \left[\text{Det}(\bar{\mathbf{A}})\right]^{-1/2} \left(A_x^2 + A_y^2\right). \quad (17)$$

It is clear from (17) that $\left[\text{Det}(\bar{\mathbf{A}})\right]^{-1/2}(A_x^2 + A_y^2)$ is independent of the frequency, thus the on-axis normalized spectrum of the electromagnetic GSM beam with or without twist phase at the imaging plane ($z = z_1 + f z_1/(z_1 - f)$) is the same as that in the source plane and is independent of the degree of polarization and other beam parameters.

If the exit plane is located at the back focal plane ($z = z_1 + f$), the transformation matrix of the total optical system between the source plane and the exit plane has the form

$$\begin{pmatrix} \mathbf{A} & \mathbf{B} \\ \mathbf{C} & \mathbf{D} \end{pmatrix} = \begin{pmatrix} \mathbf{I} & f\mathbf{I} \\ 0 & \mathbf{I} \end{pmatrix} \begin{pmatrix} \mathbf{I} & 0\mathbf{I} \\ -(1/f)\mathbf{I} & \mathbf{I} \end{pmatrix} \begin{pmatrix} \mathbf{I} & z_1\mathbf{I} \\ 0\mathbf{I} & \mathbf{I} \end{pmatrix}$$

$$= \begin{pmatrix} 0\mathbf{I} & f\mathbf{I} \\ -(1/f)\mathbf{I} & (1 - z_1/f)\mathbf{I} \end{pmatrix}. \quad (18)$$

In this case, if we set $\boldsymbol{\rho} \equiv (0\,0)$, (15) reduces to

$$S(0, z, \omega)$$

$$= \frac{\Gamma_0^2}{(\omega - \omega_0)^2 + \Gamma_0^2}$$

$$\times \left[A_x^2 \left[\text{Det}(\bar{\mathbf{B}}\mathbf{M}_{0xx}^{-1})\right]^{-1/2} + A_y^2 \left[\text{Det}(\bar{\mathbf{B}}\mathbf{M}_{0yy}^{-1})\right]^{-1/2}\right]$$

$$= \frac{\Gamma_0^2}{(\omega - \omega_0)^2 + \Gamma_0^2} \frac{4\omega^2}{f^2 c^2}$$

$$\times \left[\frac{A_x^2 \delta_{gx}^2 \sigma_x^4}{4\sigma_x^2 + \delta_{gx}^2(1 + 4\sigma_x^4 \omega^2 \gamma_{xx}^2/c^2)} \right.$$

$$\left. + \frac{A_y^2 \delta_{gy}^2 \sigma_y^4}{4\sigma_y^2 + \delta_{gy}^2(1 + 4\sigma_y^4 \omega^2 \gamma_{yy}^2/c^2)}\right]. \quad (19)$$

One finds from (19) that the on-axis normalized spectrum $S(0, z, \omega)/S(0, z, \omega)_{\max}$ of a focused electromagnetic GSM beam without twist phase ($\gamma_{xx} = \gamma_{yy} = 0$) at the back focal plane is independent of the initial degree of polarization and other beam parameters, and the maximum relative spectral shift η equals 0.03516. When $\gamma_{xx} \neq 0$ and $\gamma_{yy} \neq 0$, it is obvious from (19) that the on-axis normalized spectrum $S(0, z, \omega)/S(0, z, \omega)_{\max}$ and the maximum relative spectral shift of a focused twisted electromagnetic GSM beam are closely related to its initial degree of polarization and other beam parameters. Furthermore, we see from (19) that the on-axis spectrum of the focused electromagnetic GSM beam is independent of z_1, which is in agreement with the result derived for the case of scalar GSM beam [52–54].

Figure 5 shows the on-axis relative spectral shift η of a focused twisted electromagnetic GSM beam versus propagation distance for different values of the twist factors
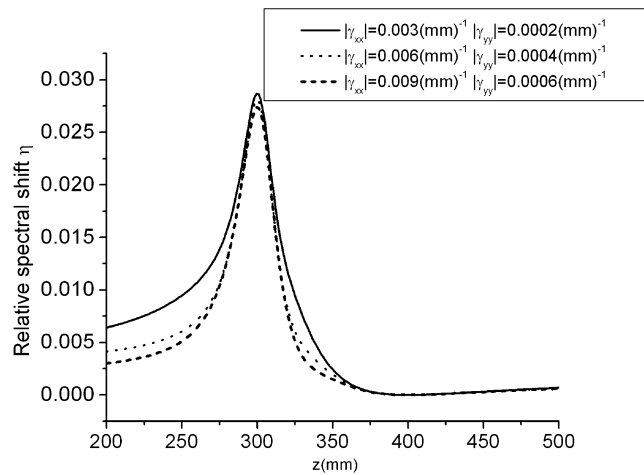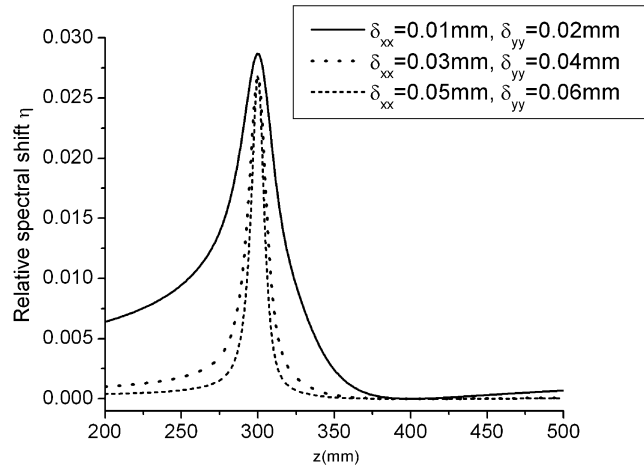

Fig. 5 On-axis relative spectral shift η of a focused twisted electromagnetic GSM beam versus propagation distance for different values of the twist factors γ_{xx} and γ_{yy} with $P_0 = 0.6$, $\delta_{xx} = 0.01$ mm and $\delta_{yy} = 0.02$ mm

Fig. 6 On-axis relative spectral shift η of a focused twisted electromagnetic GSM beam versus propagation distance for different values of the correlation coefficients of the initial beam δ_{xx} and δ_{yy} with $P_0 = 0.6$, $\gamma_{xx} = 0.006$ mm^{-1} and $\gamma_{yy} = 0.0004$ mm^{-1}

γ_{xx} and γ_{yy} with $P_0 = 0.6$, $\delta_{xx} = 0.01$ mm and $\delta_{yy} = 0.02$ mm. From Fig. 5, we find that the twist phase has significant influence on the relative spectral shift on propagation. The relative spectral shift on propagation and the maximum relative spectral shift at the back focal plane increase as the absolute values of the twist factors decrease, while a zero spectral shift still occurs at the image plane. Figure 6 shows the on-axis relative spectral shift η of a focused twisted electromagnetic GSM beam versus propagation distance for different values of the correlation coefficients of the initial beam δ_{xx} and δ_{yy} with $P_0 = 0.6$, $\gamma_{xx} = 0.006$ mm^{-1} and $\gamma_{yy} = 0.0004$ mm^{-1}. It is clear that the correlation coefficients also affect the relative spectral shift strongly. With the decrease of the correlation coeffi-
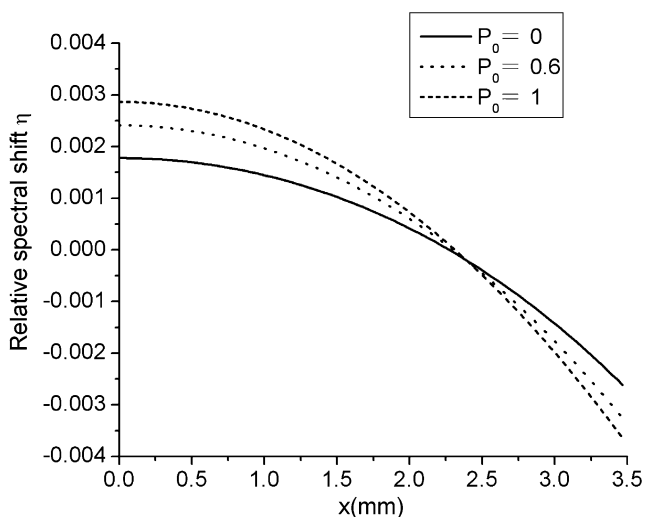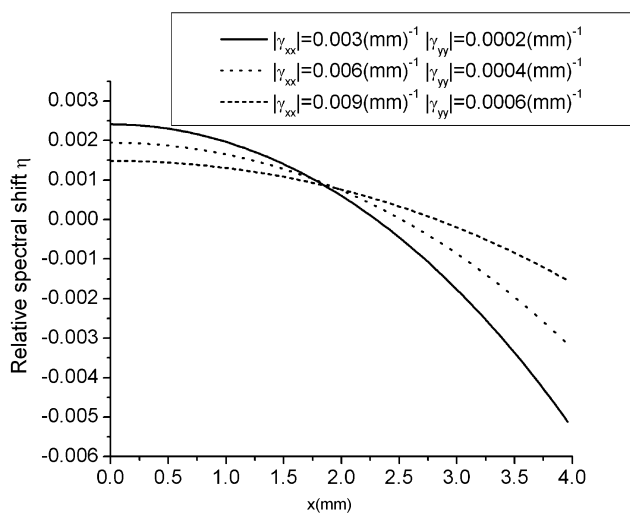
Fig. 7 Relative spectral shift of a focused twisted electromagnetic GSM beam versus the transverse coordinate x for different values of the degree of polarization of the initial beam at $z = 350$ mm with $\gamma_{xx} = 0.003$ mm^{-1}, $\gamma_{yy} = 0.0002$ mm^{-1}, $\delta_{xx} = 0.01$ mm and $\delta_{yy} = 0.02$ mm

Fig. 8 Relative spectral shift of a focused twisted electromagnetic GSM beam versus the transverse coordinate x for different values of twist factors γ_{xx} and γ_{yy} of the initial beam at $z = 350$ mm with $P_0 = 0.6$, $\delta_{xx} = 0.01$ mm and $\delta_{yy} = 0.02$ mm

cients, the relative spectral shift increases. When the values of the correlation coefficients are large, the spectral changes occur only in a small range near the back focal plane.

All above discussions are confined to the on-axis spectrum and relative spectral shift. In Fig. 7, we calculate the relative spectral shift of a focused twisted electromagnetic GSM beam versus the transverse coordinate x for different values of the degree of polarization of the initial beam at $z = 350$ mm with $\gamma_{xx} = 0.003$ mm^{-1}, $\gamma_{yy} = 0.0002$ mm^{-1}, $\delta_{xx} = 0.01$ mm and $\delta_{yy} = 0.02$ mm. In Fig. 8, we calculate the relative spectral shift of a focused twisted electromagnetic GSM beam versus the transverse coordinate x for different values of twist factors γ_{xx} and γ_{yy} of the initial beam at $z = 350$ mm with $P_0 = 0.6$, $\delta_{xx} = 0.01$ mm and $\delta_{yy} = 0.02$ mm. In Fig. 9, we calculate the relative spectral shift of a focused twisted electromagnetic GSM beam versus the transverse coordinate x for different values of the correlation coefficients δ_{xx} and δ_{yy} at $z = 350$ mm with $P_0 = 0.6$, $\gamma_{xx} = 0.003$ mm^{-1} and $\gamma_{yy} = 0.0002$ mm^{-1}. One finds from Figs. 7–9 that the relative spectral shift gradually decreases as the transverse coordinate x increases, and a red shift can be observed when x is large enough. For certain value of transverse coordinate x, no spectral shift occurs. Furthermore, the absolute value of the relative spectral shift increases as the initial degree of polarization increases, and decreases as the absolute values of initial twist factors (γ_{xx} and γ_{yy}) or initial correlation coefficients increase.
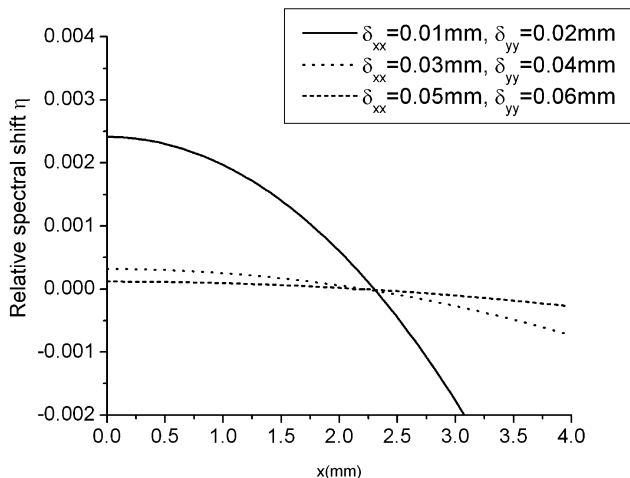

Fig. 9 Relative spectral shift of a focused twisted electromagnetic GSM beam versus the transverse coordinate x for different values of the correlation coefficients δ_{xx} and δ_{yy} at $z = 350$ mm with $P_0 = 0.6$, $\gamma_{xx} = 0.003$ mm^{-1} and $\gamma_{yy} = 0.0002$ mm^{-1}

4 Conclusion

In conclusion, we have studied the spectral shift of a twisted electromagnetic GSM beam focused by a thin lens with the help of the tensor method. Dependence of on-axis and off-axis relative spectral shifts on the degree of polarization, twist phase and correlation coefficients of the initial beam is explored numerically. We have found that the relative spectral shift of focused twisted electromagnetic GSM beam is closely determined by the initial beam's parameters, the blue shift occurs at on-axis points, while the red shift can occur at off-axis points. Our formulae and method provide a convenient way for analyzing the spectrum properties of elec-

tromagnetic GSM beam with or without twist phase passing through paraxial optical system.

References

1. L. Mandel, E. Wolf, *Optical Coherence and Quantum Optics* (Cambridge University Press, Cambridge, 1995)
2. P.D. Santis, F. Gori, G. Guattari, C. Palma, Opt. Commun. **29**, 256 (1979)
3. F. Gori, Opt. Commun. **34**, 301 (1980)
4. A.T. Friberg, R.J. Sudol, Opt. Commun. **41**, 383 (1982)
5. A.T. Friberg, J. Turunen, J. Opt. Soc. Am. A **5**, 713 (1988)
6. F. Wang, Y. Cai, J. Opt. Soc. Am. A **24**, 1937 (2007)
7. E. Tervonen, A.T. Friberg, J. Turunen, J. Opt. Soc. Am. A **9**, 796 (1992)
8. R. Simon, N. Mukunda, J. Opt. Soc. Am. A **10**, 95 (1993)
9. R. Simon, N. Mukunda, J. Opt. Soc. Am. A **15**, 2373 (1998)
10. A.T. Friberg, E. Tervonen, J. Turunen, J. Opt. Soc. Am. A **11**, 1818 (1994)
11. D. Ambrosini, V. Bagini, F. Gori, M. Santarsiero, J. Mod. Opt. **41**, 1391 (1994)
12. R. Simon, A.T. Friberg, E. Wolf, Pure Appl. Opt. **5**, 331 (1996)
13. M.J. Bastiaans, J. Opt. Soc. Am. A **17**, 2475 (2000)
14. P. Östlund, A.T. Friberg, Opt. Rev. **8**, 1 (2001)
15. Q. Lin, Y. Cai, Opt. Lett. **27**, 216 (2002)
16. Q. Lin, Y. Cai, Opt. Lett. **27**, 1672 (2002)
17. Y. Cai, Q. Lin, D. Ge, J. Opt. Soc. Am. A **19**, 2036 (2002)
18. Y. Cai, Q. Lin, Opt. Commun. **211**, 1 (2002)
19. Y. Cai, L. Hu, Opt. Lett. **31**, 685 (2006)
20. Y. Cai, S. He, Appl. Phys. Lett. **89**, 041117 (2006)
21. Y. Cai, U. Peschel, Opt. Express **15**, 15480 (2007)
22. Y. Cai, Q. Lin, O. Korotkova, Opt. Express **17**, 2450 (2009)
23. D.F.V. James, J. Opt. Soc. Am. A **11**, 1641 (1994)
24. F. Gori, Opt. Lett. **23**, 241 (1998)
25. G.P. Agrawal, E. Wolf, J. Opt. Soc. Am. A **17**, 2019 (2000)
26. F. Gori, M. Santarsiero, G. Piquero, R. Borghi, A. Mondello, R. Simon, J. Opt. A, Pure Appl. Opt. **3**, 1 (2001)
27. G. Piquero, F. Gori, P. Romanini, M. Santarsiero, R. Borghi, A. Mondello, Opt. Commun. **208**, 9 (2002)
28. E. Wolf, Phys. Lett. A **312**, 263 (2003)
29. Y. Cai, D. Ge, Q. Lin, J. Opt. A, Pure Appl. Opt. **5**, 453 (2003)
30. O. Korotkova, M. Salem, E. Wolf, Opt. Lett. **29**, 1173 (2004)
31. D. Ge, Y. Cai, Q. Lin, Chin. Phys. **14**, 128 (2005)
32. E. Wolf, *Introduction to the Theory of Coherence and Polarization of Light* (Cambridge University Press, Cambridge, 2007)
33. T. Shirai, O. Korotkova, E. Wolf, J. Opt. A, Pure Appl. Opt. **7**, 232 (2005)
34. F. Gori, M. Santarsiero, R. Borghi, V. Ramírez-Sánchez, J. Opt. Soc. Am. A **25**, 1016 (2008)
35. B. Kanseri, H.C. Kandpal, Opt. Lett. **33**, 2410 (2008)
36. O. Korotkova, Opt. Commun. **281**, 2342 (2008)
37. M. Yao, Y. Cai, H.T. Eyyuboğlu, Y. Baykal, O. Korotkova, Opt. Lett. **33**, 2266 (2008)
38. O. Korotkova, M. Yao, Y. Cai, H.T. Eyyuboğlu, Y. Baykal, J. Opt. Soc. Am. A **25**, 2710 (2008)
39. Z. Tong, O. Korotkova, Y. Cai, H.T. Eyyuboğlu, Y. Baykal, Appl. Phys. B **97**, 849 (2009)
40. Y. Cai, O. Korotkova, H.T. Eyyuboğlu, Y. Baykal, Opt. Express **16**, 15835 (2008)
41. O. Korotkova, Y. Cai, E. Watson, Appl. Phys. B **94**, 681 (2009)
42. Y. Cai, O. Korotkova, Appl. Phys. B **96**, 499 (2009)
43. C. Zhao, Y. Cai, O. Korotkova, Opt. Express **17**, 21472 (2009)
44. E. Wolf, Phys. Rev. Lett. **56**, 1370 (1986)
45. E. Wolf, Nature **326**, 363 (1987)
46. F. Gori, G.L. Marcopoli, M. Santarsiero, Opt. Commun. **81**, 123 (1991)
47. M. Santarsiero, F. Gori, Phys. Lett. A **167**, 123 (1991)
48. E. Wolf, D.F.V. James, Rep. Prog. Phys. **59**, 771 (1996)
49. C. Palma, G. Cardone, G. Cincotti, IEEE J. Quantum Electron. **34**, 1082 (1998)
50. J. Pu, H. Zhang, S. Nemoto, Opt. Commun. **162**, 57 (1999)
51. Y. Cai, Q. Lin, Opt. Commun. **204**, 17 (2002)
52. C. Palma, G. Cincotti, Opt. Lett. **22**, 671 (1997)
53. C. Palma, G. Cincotti, G. Guattari, J. Quantum Electron. **34**, 378 (1998)
54. Y. Cai, Y. Huang, Q. Lin, J. Opt. A, Pure Appl. Opt. **5**, 397 (2003)
55. H. Roychowdury, G.P. Agrawal, E. Wolf, J. Opt. Soc. Am. A **23**, 940 (2006)
56. J. Pu, O. Korotkova, E. Wolf, Opt. Lett. **31**, 2097 (2006)
57. J. Pu, O. Korotkova, E. Wolf, Phys. Rev. E **75**, 056610 (2007)
58. O. Korotkova, J. Pu, E. Wolf, J. Mod. Opt. **55**, 1199 (2008)